Supplementary Information

Examining iron complexes with organic ligands by laboratory XAFS

Damian Motz,*[a]††§ Sebastian Praetz,[b]§ Christopher Schlesiger,[b] Jonathan Henniges,[a] Florian Böttcher,[a] Bernhard Hesse,[c]††† Hiram Castillo-Michel,[c] Steven Mijatz,[c] Wolfgang Malzer,[b] Birgit Kanngießer [b] and Carla Vogt *[a]††††

a: Leibniz University Hannover, Institute of Inorganic Chemistry, Callinstraße 1, 30167 Hannover, Germany.
b: *Technical University Berlin, Institute for Optics and Atomic Physics, Sekr. EW 3-1, Hardenbergstraße 36, 10623 Berlin, Germany.*
c: *European Synchrotron Radiation Facility, 71 avenue des Martyrs, CS 40220, 38043 Grenoble Cedex 9, France.*
††: current affiliation: Leibniz University Hannover, Institute of Building Materials Science, Appelstraße 9a, 30167 Hannover, Germany
†††: current affiliation: Xploraytion GmbH, Bismarckstrasse 10-12, 10625 Berlin, Germany.
††††: current affiliation: TU Bergakademie Freiberg, Institute of Analytical Chemistry, Leipziger Straße 29, 09599 Freiberg, Germany.
***:** d.a.motz@baustoff.uni-hannover.de, Carla.Vogt@chemie.tu-freiberg.de
§: These authors contributed equally to this work.

Syntheses of the iron(II) bzimpy complex compounds

The here applied attuned method for the synthesis of the free ligand bzimpy (**3**) based upon the original approach of Addison & Burke 1981[1] (stated yield: 53%) and the synthesizing method used by Li et al. 2008 [2] (stated yield: 79%). The following steps of preparing the coordination compounds $[Fe(bzimpy)_2](ClO_4)_2 \cdot 0.25\ H_2O$ and $[Fe(bzimpy_{-1H})_2] \cdot H_2O$ containing the complexes **4** and **5** (Scheme S2) were built on the synthesizing techniques depicted in Boča et al. 1997 [3] (stated yield of $[Fe(bzimpy)_2](ClO_4)_2 \cdot 0.25\ H_2O$: 61%), Boča et al. 2005 [4] (stated yield of $[Fe(bzimpy_{-1H})_2] \cdot H_2O$: 83%) as well as Strauß et al. 1992 [5] and Strauß et al. 1993 [6]. The syntheses of both compounds were especially optimized for an improved oxidation protection of the iron(II), as well in the sort of the solved Fe^{2+} cations as the formed iron(II) complexes, and elimination / reduction of possible iron(III) impurities. Therefore, in supplement to the addition of catalytic amounts of ascorbic acid to the reaction solution an inert gas atmosphere (for both synthesis and storage of the products in particular, although both complexes were described as relatively stable iron(II) complexes in the literature) and degassed solvents (if possible and useful – especially if the solvents where taken from an already opened bottle) were used.

2,6-Bis(benzimidazol-2-yl)pyridine (bzimpy)

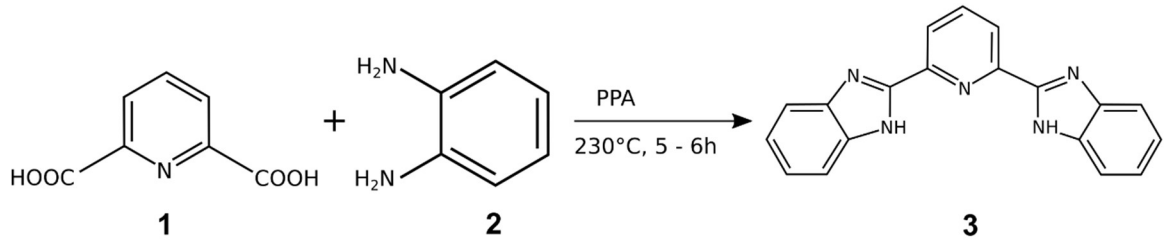

Scheme S1 Synthesis of 2,6-Bis(benzimidazol-2-yl)pyridine (bzimpy).

3.35 g pyridine-2,6-dicarboxylic acid (**1**), 4.7 g o-phenylenediamine (**2**) and 160 g polyphosphoric acid (115% or 105% PPA) were stirred in a 250 mL three-necked flask under reflux for 5 – 6 h at 230 °C. Although water is one of the bzimpy formation´s reaction products, a drying tube (containing anhydrous $CaCl_2$) was also placed on the used condenser protecting the moisture sensitive compound **2** and the PPA against water due to humidity before the reaction had been started. Despite the potential air sensitivity of compound **2** the synthesis was not done under inert gas, but no significant differences or issues in the final product yields / purities were observed. After the obtained dark green melt had been cooled at room temperature to about 150 °C it was poured into 1 L of ice water (high-purity water‡) under stirring, which resulted in the formation of a flaky blue solid. While stirring severely the acidic mixture the pH of the solution was attuned to pH 7 – 9 by adding ammonia solution

‡ In all of the described syntheses only high-purity water was used.

($\omega_{rel}(NH_3)$ ≈ 30 – 33%). During this procedure the color of the solid changed gradually from blue to green and finally to pale pink (or ocher). After this the solid was filtered off by a suction filter and washed with pure water three to four times (depended on the measured pH value in the Büchner funnel which should be at pH = 7) to remove phosphates and possible excess ammonia. The obtained pale pink or light ocher colored raw product was dried under vacuum in a desiccator for 1 – 2 d. The almost completely dry raw substance was recrystallized twice under reflux in methanol and with the addition of activated carbon. In both of the recrystallization steps the precipitation of the purified product was achieved by reducing (rotary evaporator) the solvent of the filtered (the hot solution must be filtered to remove the carbon) solution in a first step and cooling of this reduced solution by ice (or freezing mixtures like ice-water, ice-water-NaCl or ice-ethanol to get slightly higher yields) in a second step. The precipitated solid was filtered off, washed carefully (dropwise) with small amounts of cool methanol and dried under vacuum overnight. 4 – 5.2 g (yield: 60 – 83%) of pure bzimpy (**3**) were obtained as a white, powdery (in part bulky) and readily methanol soluble solid.
^{1}H-NMR (δ in ppm) in DMSO-D_6 at 400 MHz: 13.02 (br, 2 H), 8.35 (d, 2 H), 8.18 (t, 1 H), 7.76 (m, 4 H), 7.32 (m, 4 H); ESI-MS (in methanol): $[M+H]^+$ *m/z* = 312.1248 (Single Mass Analysis determined molecular formula: $C_{19}H_{14}N_5$) und $[M+Na]^+$ *m/z* = 334.1069 (Single Mass Analysis determined molecular formula: $C_{19}H_{13}N_5Na$); ATR-IR ($\tilde{\nu}$ in cm^{-1}) selected bands: ≈ 3500 – 2600, 1600, 1570, 1456, 1434, 1377, 1317, 1276, 1230, 820, 730.

$[Fe(bzimpy)_2](ClO_4)_2 \cdot 0.25\ H_2O$ and $[Fe(bzimpy_{-1H})_2] \cdot H_2O$

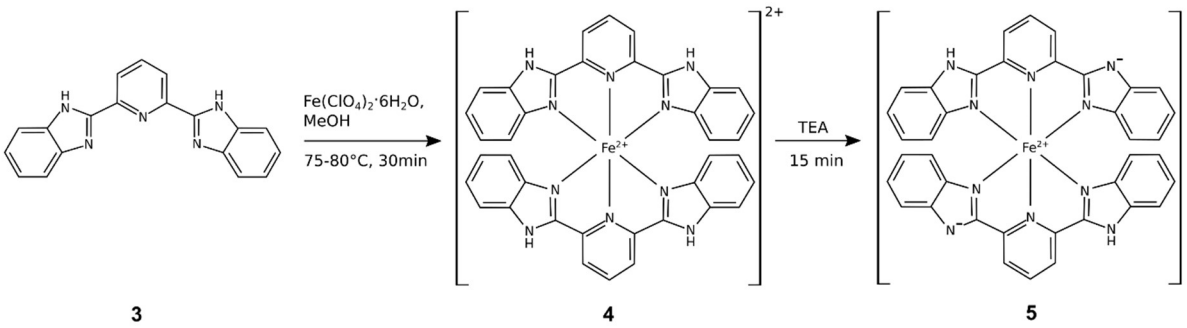

Scheme S2 Synthesis of the iron(II) bzimpy complexes.

Under argon atmosphere 0.18 g iron(II) perchlorate hydrate (as a hexahydrate: 0.5 mmol) and a spatula tip of ascorbic acid were solved in about 6 mL of a (if necessary ultra-sonic degassed) methanol-water-mixture (methanol : water = 1 : 1) in a 250 mL three-necked flask under stirring and heating (under reflux) to boil. Simultaneously 0.31 g of compound **3** were dissolved in another flask in 20 – 25 mL of a methanol-water-mixture (methanol : water = 9 : 1) under stirring and heating. The resulting hot solution of **3** was added to the warm green-yellow iron(II) solution in 5 mL steps by the use of a syringe. The reaction mixture´s color changed to wine-red or red-violet immediately and therefore indicating the formation of the iron(II) bzimpy complex **4**. After the whole ligand solution had been added, the mixture was further stirred and heated at 75 °C under argon atmosphere for 30 min. The resulting solution was the starting point of the formation of both desired products, which means either $[Fe(bzimpy)_2](ClO_4)_2 \cdot 0.25\ H_2O$ or $[Fe(bzimpy_{-1H})_2] \cdot H_2O$ was prepared from this solution.

$[Fe(bzimpy)_2](ClO_4)_2 \cdot 0.25\ H_2O$. To isolate the complex **4** as the desired ionic compound $[Fe(bzimpy)_2](ClO_4)_2 \cdot 0.25\ H_2O$, the reaction mixture was cooled at room temperature and finally by an ice bath (in later runs also the solvent was slightly reduced by rotary evaporator before the cooling to enhance the product yields). The formed solid was filtered off by a suction filter, gently (dropwise) washed with small amounts of cold (ice cooling) methanol and dried in a desiccator under vacuum overnight. $[Fe(bzimpy)_2](ClO_4)_2 \cdot 0.25\ H_2O$ was received as a wine-red / purple and fine or coarse crystalline solid in yields of 54% – 80% (on average: 73%, correspond to 0.32 g of the product) and stored under inert gas (argon).

$[Fe(bzimpy_{-1H})_2] \cdot H_2O$. To get the neutral complex **5** and isolate this deprotonated species as the compound $[Fe(bzimpy_{-1H})_2] \cdot H_2O$, 10.2 mL of a triethylamine solution in methanol (0.21 mL TEA in 10 mL methanol) were added to the hot reaction mixture by a syringe. The mixture´s color changed from wine-red to dark blue instantly and indicated the deprotonation of **4** and formation of **5**. The blue solution was stirred and heated to 75 °C under argon for further 15 min. The precipitation, the filtering off, washing and drying of the product were done similarly to $[Fe(bzimpy)_2](ClO_4)_2 \cdot 0.25\ H_2O$ (see above). Finally $[Fe(bzimpy_{-1H})_2] \cdot H_2O$ was achieved as a dark blue and fine powdery solid in yields of 48% – 90% (on average: 79%, correspond to 0.27 g of the product) and also stored under argon.

Synthesis of iron(III) meso-tetraphenylporphyrin chloride (FeTPP(Cl))

To prepare the free porphyrin TPP (**8**) via the simple, fast and therefore very common Adler-Longo reaction in the first synthesis step, a method which based directly on the original approach of Adler et al. 1967 [7] (stated TPP yield: 20%) was developed and attuned. Besides the relatively low yields and limited accessible substituted porphyrins [8–11] one of the Adler-method´s major disadvantages are small but not negligible chlorine impurities of the product (3% TPC (**9**) in case of TPP synthesis [7], 2% - 10% in general [9,12]), due to an *in-situ* reduction of the already formed porphyrin under the Adler-Longo reaction conditions [13]. To minimize these chlorine contents the raw TPP was treated with a chemical clean-up technique based on the subsequent chlorine content´s oxidation by DDQ presented in Rousseau & Dolphin 1974 [13] and Barnett et al. 1975 [12]. The effort of this purification method could easily be checked by UV-Vis spectroscopy by determining the ratios between the Q bands Q_4 and Q_3 (band areas and / or absorption maxima). As it is mentioned by Rousseau & Dolphin 1974 [13] TPC containing raw TPP exhibits a ratio of $Q_4/Q_3 > 0.75$ in DCM whereas pure TPP shows $Q_4/Q_3 = 0.75$ in the same solvent. The metalation of the free ligand **8** and thus preparation of FeTPP(Cl) (**10**) in a second synthesis step was done by a developed method based on the descriptions in Adler et al. 1970[14] (stated yield for several metal porphyrins in general: up to 100%) as well as especially Fleischer et al. 1971[15] (stated FeTPP(Cl) yield: 70% – 80%) and Sun et al. 2011 [11] (stated FeTPP(Cl) yield: up to 97.4%).

It has to be mentioned that several other porphyrins and their associated iron(III) porphyrin chlorides were also synthesized successfully, characterized and finally used in the laboratory XAFS experiments in part of this work (see Motz 2021 [16]). Especially the chloro-, methyl-, methoxy- and carboxy-substituted meso-tetraphenylporphyrins TClPP, TMePP, TMxPP and TCPP and their complexes FeTClPP(Cl), FeTMePP(Cl), FeTMxPP(Cl) and FeTCPP(Cl), but also the β-substituted porphyrin OEP and FeOEP(Cl) were synthesized successfully by slightly, but specifically attuned syntheses prescriptions based on the TPP (but without the attached additional DDQ treatment) and FeTPP(Cl) syntheses described hereinafter. Just the synthesis of the free base OEP required a different method in sort of a classical Rothemund reaction as it is e.g. described for the methyl analogue OMP by Cheng & LeGoff 1977 [17]). The results for these other iron(III) porphyrins are not yet presented here, because the obtained laboratory XAFS spectra for these different iron(III) porphyrins were only partially distinguishable (due to their distinctive structural similarities [16]) and further laboratory XAFS measurements / improvements (as well as additional synchrotron XAFS measurements) are necessary to get more meaningful results for them.

Meso-Tetraphenylporphyrin (TPP)

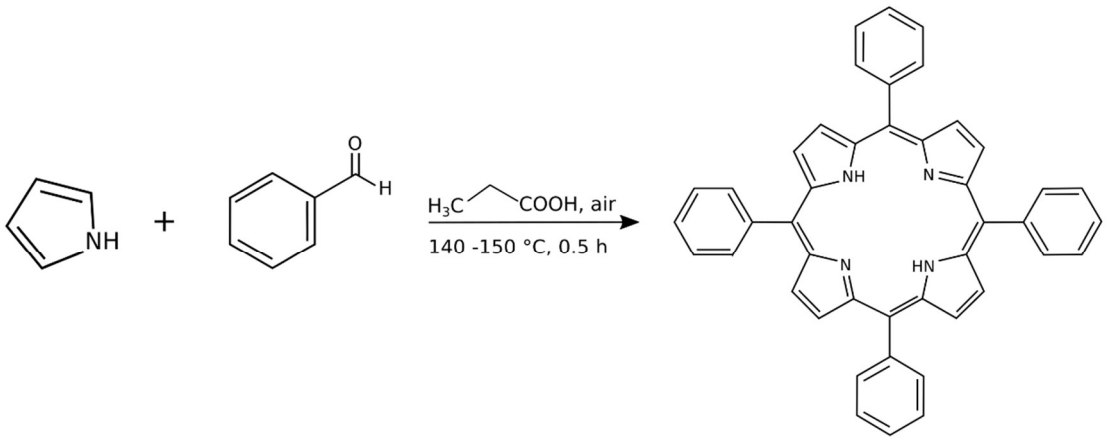

Scheme S3 Synthesis of meso-Tetraphenylporphyrin (TPP).

Raw product synthesis. 16 mL benzaldehyde (**7**) and ca. 600 mL propionic acid were mixed in a 1 L three-necked flask, stirred and heated under reflux up to 140 °C – 150 °C. By syringe 11.2 mL fresh pyrrole (**6**) were added to the boiling solution. The mixture colored to brown-red (or brown-violet) directly and was stirred and heated for further 30 min. This increased the color´s intensity even more and it resulted in a dark brown-violet (or green) solution. After the reaction mixtures had been cooled down to room temperature (just by air cooling), a more intensive cooling by an ice bath (for ca. 15 min) was applied and a precipitation of large amounts of a dark solid was observed. This solid was filtered off by suction filter and washed with large quantities of hot (boiling) water (at least 200 mL – 300 mL) and finally some drops of cold (ice bath) methanol to remove

the remains of propionic acid, educts **6** and **7** and several byproducts of the reaction. The solid product was dried in a desiccator under vacuum overnight. TPP (**8**) was obtained as a raw product in the form of a dark violet, fine crystalline solid in yields of 14% - 21% (ca. 3.4 g – 5.1 g raw TPP).

^{1}H-NMR (δ in ppm) in $CDCl_3$ at 400 MHz: 8.88 (s, 8 H), 8.25 (d, 8 bzw. 9 H), 7.77 (2x d, 12 H), -2.73 (s, 2 H); ESI-MS (in methanol): $[M+H]^+$ m/z = 615.2545 Da (Single Mass Analysis determined molecular formula: $C_{44}H_{31}N_4$); ATR-IR ($\tilde{\nu}$ in cm^{-1}) selected bands: 3316, 3055, 1595, 1348, 964, 732; UV-Vis in DCM (λ_{max} in nm): 415 (Soret), 514, 549, 590, 645; Q_4/Q_3: ≈ 0,87.

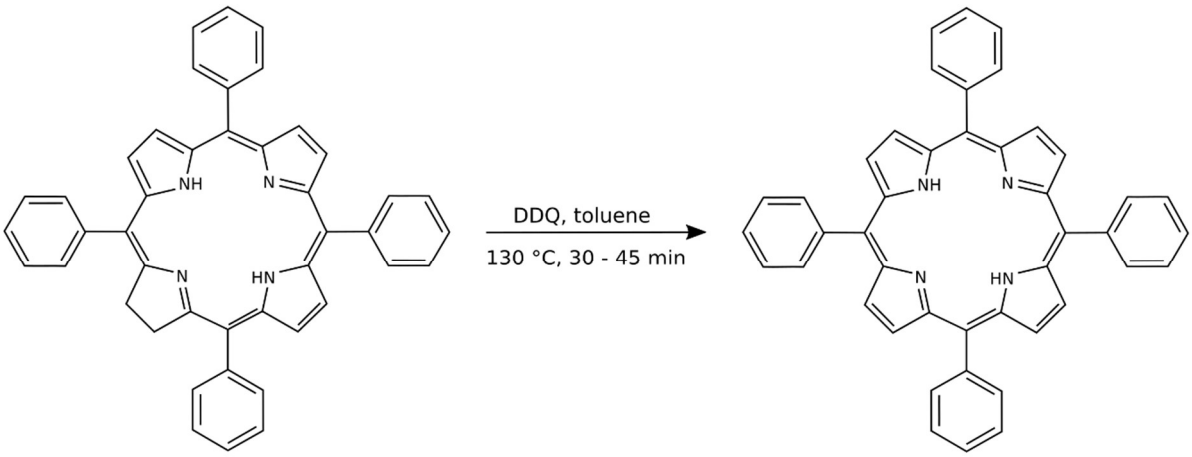

9 **8**

Scheme S4 Purification of TPP.

Raw product purification. To remove the mentioned small contents of chlorine (meso-tetraphenylchlorine, TPC, **9**) from the raw product for getting a much purer product the chemical clean-up by chlorine oxidation was applied. 3.3 g raw TPP (**8**) were dissolved in about 500 mL toluene, mixed with 0.825 g DDQ (2,3-Dichloro-5,6-dicyano-1,4-benzoquinone) and heated under stirring and reflux up to 130 °C for 30 min – 45 min. After the dark red reaction mixture had been cooled down to room temperature, it was treated with 500 mL alkaline sodium dithionite solution (0.5 g $Na_2S_2O_4$ in 500 mL NaOH solution, ω_{rel}(NaOH) = 1%) in a separating funnel. Two separated phases were obtained (the phase boundary was difficult to spot due to the intensive dark colors) – an organic phase in the sort of a dark red solution and a yellow-greenish, solid containing aqueous phase. After it had been separated, the organic phase was washed three-times with 100 mL water each and dried by anhydrous sodium sulfate. Finally, the solvent was removed completely by rotary evaporator and a dark violet solid remained. This solid was dissolved (or suspended) in small amounts (40 mL maximally) of a cold DCM-methanol mixture (DCM : methanol = 1 : 1). The solution / suspension was cooled in a freezing mixture (ice-ethanol or ice-water-NaCl) for 30 min – 45 min. The resulting solid was filtered off by suction filter, washed with hot water and finally some drops of cold methanol and dried under vacuum overnight. The purified TPP (**8**) was obtained as a violet (coarsy) crystalline solid in yields of 58% - 87% (much depending on the used amounts of DCM-methanol mixture, the cooling time and the amounts of methanol to wash the solid) and was stored in the dark at 4 °C (laboratory refrigerator).

^{1}H-NMR (δ in ppm) in $CDCl_3$ at 400 MHz: 8.87 (s, 8 H), 8.24 (d, 8 or 9 H), 7.77 (2x d, 12 H), -2.74 (s, 2 H); ESI-MS (in methanol): $[M+H]^+$ m/z = 615.2552 Da (Single Mass Analysis determined molecular formula: $C_{44}H_{31}N_4$); ATR-IR ($\tilde{\nu}$ in cm^{-1}) selected bands: 3313, 3055, 1593, 1348, 964, 732; UV-Vis in DCM (λ_{max} in nm): 415 (Soret), 514, 549, 590, 645; Q_4/Q_3: ≈ 0,71.

Iron(III) meso-tetraphenylporphyrin chloride (FeTPP(Cl))

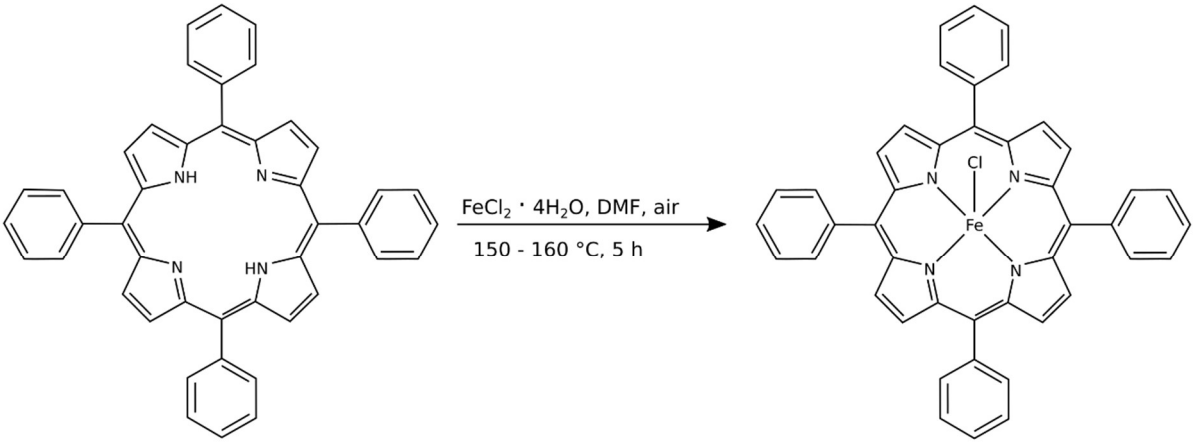

8 **10**

Scheme S5 Synthesis of iron(III) meso-tetraphenylporphyrin chloride (FeTPP(Cl)).

1 g purified **8** and 1.94 g iron(II) chloride tetrahydrate were dissolved in 100 mL DMF in a 250 mL two-necked flask and heated under stirring and reflux up to 150 °C – 160 °C for 5 h. Afterwards the dark orange-red (or brown) solution was cooled down to about 60 °C at room temperature and the solvent was reduced by half (rotary evaporator). While standing in an ice bath this reduced solution was mixed with 40 mL of 6 M hydrochloric acid under slightly shaking as well to increase the chloride concentration as to inhibit the formation of possible hydroxo or oxo dimers of the iron porphyrin (TPP-Fe-O-FeTPP). After the developing heat and fumes had decreased, the dark green-brown and cloudy solution was cooled by the ice bath for further 5 min. Subsequently the precipitated solid was filtered off by suction filter and washed at least three-times with 40 mL 3 M hydrochloric acid each (the filtrates' color should change from yellow-brown to colorless) to remove the unreacted excess of iron(III). The solid was vacuum dried for 1 d – 2 d and the resulting raw FeTPP(Cl) (**10**) was obtained in the sort of a blue-violet solid containing visible amounts of a red-brown powder, which was identified as iron(III) oxide by XRD. To remove this by-product the raw FeTPP(Cl) was recrystallized under reflux in xylene (the hot FeTPP(Cl) solution was filtered to delete the insoluble iron oxide). After the solvent had been removed completely, the remaining solid was dissolved (suspended) in a small amount (max. 45 mL, optimum 10 mL – 15 mL) of a DCM-methanol mixture (DCM : methanol = 1 : 2). This suspension/ solution was cooled by an ice-ethanol-bath for 15 min and the resulting precipitated solid was filtered off without further cleaning. After drying under vacuum overnight 0.7 g – 1.1 g purified blue-violet and fine crystalline FeTPP(Cl) (**10**) was received (yield: 62% – 86%) and was stored in the dark at 4 °C (laboratory refrigerator).

Characterization of $[Fe(bzimpy)_2](ClO_4)_2 \cdot 0{,}25\ H_2O$, $[Fe(bzimpy_{-1H})_2] \cdot H_2O$ and FeTPP(Cl)

Speciation

Speciation to identify the synthesized iron complexes as well as to get an information on their purity was done by UV-Vis and IR spectroscopy. UV-Vis spectra were obtained in methanol (iron(II) bzimpy complexes) or DCM (TPP and FeTPP(Cl)) solutions in quartz glass cuvettes (d = 1 cm) by the use of an *UV-1600 PC Spectrophotometer* (*VWR*, Radnor, USA) at its highest resolution / increment of 0.1 nm. For IR spectroscopy attenuated total reflection (ATR) IR with a spectrometer type *Tensor 27* (*Bruker Corporation*, Billerica, USA) was used. Fig. S1 a - d presents the obtained spectra and in Table S1 the most important observed bands are shown in comparison to literature values.

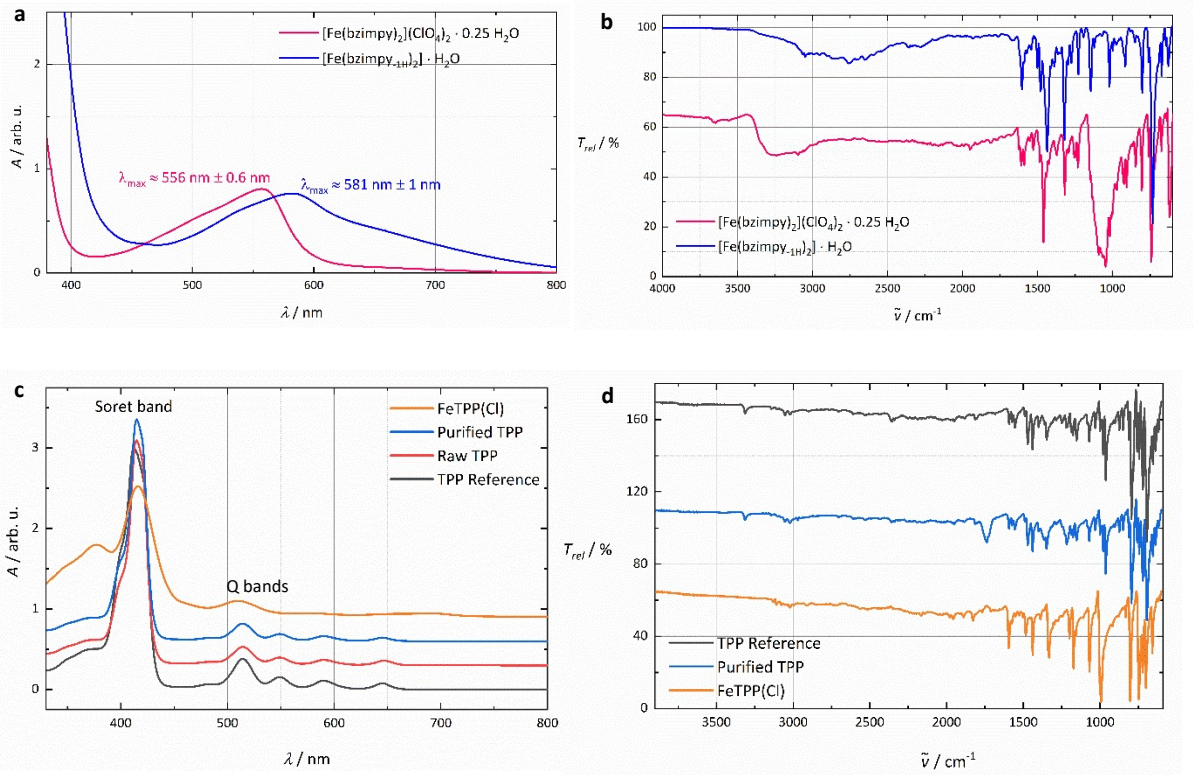

Fig. S1 Speciation results of the synthesized iron complexes - **a** UV-Vis spectra of $[Fe(bzimpy)_2](ClO_4)_2 \cdot 0.25\ H_2O$ (wine red) and $[Fe(bzimpy_{-1H})_2] \cdot H_2O$ (blue) in methanol at $c = 10^{-4}$ mol/L (quoted absorption maxima are the averages of different synthesized product charges), **b** ATR-IR spectra of $[Fe(bzimpy)_2](ClO_4)_2 \cdot 0.25\ H_2O$ (wine red) and $[Fe(bzimpy_{-1H})_2] \cdot H_2O$ (blue) (spectra offset), **c** UV-Vis spectra of the reference TPP (black), raw TPP (red), purified (chlorine free) TPP (blue) and FeTPP(Cl) (orange) in DCM at $c = 10^{-5}$ mol/L (spectra offset), **d** ATR-IR spectra of the reference TPP (black), purified TPP (blue) as well as FeTPP(Cl) (orange) (spectra offset).

Table S1 Overview of the most important obtained speciation results compared to the literature.

Sample	Observed bands	Literature
$[Fe(bzimpy)_2](ClO_4)_2 \cdot 0.25\ H_2O$	UV-Vis in MeOH: $\lambda_{max} \approx 556$ nm ± 0.6 nm	UV-Vis in MeOH: $\lambda_{max} = 557$ nm [6] (in general $\lambda_{max} \approx 550$ nm [5], depending on concentration and exact ratios between iron(II) and the ligand bzimpy)
$[Fe(bzimpy_{-1H})_2] \cdot H_2O$	UV-Vis in MeOH: $\lambda_{max} \approx 581$ nm ± 1nm, wider band	UV-Vis in MeOH: λ_{max} shift to longer wavelength and broadening of the band [5]
Reference TPP (*Sigma Aldrich*)	UV-Vis in DCM: 418 nm, 514 nm, 549 nm, 590 nm, 645 nm	UV-Vis in DCM: 417 nm (Soret), 514 nm (Q_1), 538 nm (Q_2), 585 nm (Q_3), 620 nm or 645 nm (Q_4) [5,11]
	ATR-IR: 3313 cm^{-1}, 3055 cm^{-1}, 1593 cm^{-1}, 1348 cm^{-1}, 962 cm^{-1}, 732 cm^{-1}	KBr: 3309 cm^{-1} (ν(N-H)), 3051 cm^{-1}, 1594 cm^{-1}, 1352 cm^{-1}, 966 cm^{-1} (δ(N-H)), 732 cm^{-1} [11]
TPP (purified)	UV-Vis in DCM: 415 nm, 514 nm, 549 nm, 590 nm, 645 nm	v. s.
	ATR-IR: 3313 cm^{-1}, 3055 cm^{-1}, 1593 cm^{-1}, 1348 cm^{-1}, 964 cm^{-1}, 732 cm^{-1}	v. s.
FeTPP(Cl)	UV-Vis in DCM: 416 nm, 510 nm, 577 nm (, 691 nm)	UV-Vis in DCM: 418 nm (Soret), 507 nm (Q), 572 nm (Q) [11]
	ATR-IR: 2923 cm^{-1}, 1595 cm^{-1}, 1332 cm^{-1}, 993 cm^{-1}, 748 cm^{-1}	KBr: 2923 cm^{-1}, 1597 cm^{-1}, 1340 cm^{-1}, 991 cm^{-1} (ν(Fe-N)), 750 cm^{-1}, 379 cm^{-1} (ν(Fe-Cl)) [11]

In case of $[Fe(bzimpy)_2](ClO_4)_2 \cdot 0.25\ H_2O$ a strong and relatively broad absorption band (Fig. S1a) with an absorption maximum at $\lambda_{max} \approx 556$ nm was observed. This value and band structure fitted to literature information [5,6] as well as to the physical background of the sample´s electromagnetic radiation absorption due to possible d-d transitions (octahedral coordination, in ground state ls-$3d^6$: transition $t_{2g}^6e_g^0 \rightarrow t_{2g}^5e_g^1$ or $^1A \rightarrow {}^1T$) and especially charge transfer effects (metal to ligand charge transfer) [5,6,18–20] very well. The same applied to $[Fe(bzimpy_{-1H})_2] \cdot H_2O$ (Fig. S1a). In relation to $[Fe(bzimpy)_2](ClO_4)_2 \cdot 0.25\ H_2O$ the shift and broadening of the absorption band described in literature [5] was clearly observed. The evaluations of the IR spectra (Fig. S1b) were mainly focused on the perchlorate stretching vibration at $\tilde{\nu} \approx 1075 - 1140\ cm^{-1}$ [21]. As expected, this band appeared in the spectrum of $[Fe(bzimpy)_2](ClO_4)_2 \cdot 0.25\ H_2O$ but not in that of $[Fe(bzimpy_{-1H})_2] \cdot H_2O$. The speciation of the FeTPP(Cl) was done in an even more detailed manner, because the free ligand TPP also exhibits a meaningful UV-Vis spectrum as well as the commercial available TPP (received from *Sigma Aldrich*) which was used as a reference. So, the synthesized iron porphyrin was analyzed in direct comparison to its synthesized preliminary stages, the raw TPP and purified TPP, as well to the reference TPP. The UV-Vis spectrum (Fig. S1c) of the synthesized and purified TPP incorporated the porphyrin typical very intensive Soret band at $\lambda \approx 400$ nm (allowed π-π* transitions) and the weaker and constantly decreasing

Q bands (partially allowed π-π* transitions) [11,13,22–25] and was in good accordance to the reference TPP as well as the literature [5,11]. The same was the case with the obtained IR spectrum, although the lower resolution of the used ATR technique and the resulting less informative spectra had to be considered for comparing to the selected literature values [11]. The synthesized FeTPP(Cl) exhibited an UV-Vis spectrum containing a slightly shifted and broadened Soret band as well as a reduced number of Q bands (TPP: four Q bands, FeTPP(Cl): two Q bands), because in case of such iron porphyrins the physical backgrounds of electromagnetic radiation absorption are a combination of the mentioned absorption properties of the ligand as well as the coordinated metal cation (d-d transitions, CT transitions, between the iron(III)´s 3d-electrons and the macrocyclic π-band etc.) [11,23–25]. The obtained bands fitted to the literature [11] well. The same accordance with the literature and theory was observed for the obtained IR spectrum of FeTPP(Cl) (Fig. S1d), as it can be seen in the loss of the N-H bands ($\tilde{\nu}$ = 3309 cm^{-1}, 966 cm^{-1}) but the emergence of Fe-N stretching vibration band ($\tilde{\nu}$ = 993 cm^{-1}). The Fe-Cl band (literature [11]: $\tilde{\nu}$ = 379 cm^{-1}) could not be observed due to the fact that the ATR technique with a limited measuring range ($\tilde{\nu}$ = 4000 – 600 cm^{-1}) was used.

Elemental analysis

In addition to the speciation an elemental analysis was done. These quantitative analyses were performed with an ICP-OES *Spectro ARCOS* (*Spectro Analytical Instruments GmbH*, Kleve, Germany). The focus of these measurements was just on the quantification of the samples iron contents, because these determined values also allowed confirming the identity and purity of the synthesized iron compounds. The quantified iron contents were also important for estimating the sample amounts for the XAFS preparations more precisely to get pellets of optimal / useable area densities *Q*. Other metals were not analyzed due to the general low content of iron in the considered iron complexes. Therefore, possible impurities like other trace metals introduced during the syntheses (e.g. due to used educts, especially iron(II) perchlorate and chloride) were not expected to be significant in the XAFS experiments.
At first the three synthesized iron compounds were dissolved or at least demetallized by microwave assisted digestion (microwave assisted digestion system *µPREP-A*, *MLS GmbH*, Leutkirch, Germany) in aqua regia (HCl : HNO_3 = 3 : 1). The acids which were used to obtain this digestion medium were p. a. sub boiled nitric acid ($\omega_{rel.}(HNO_3)$ = 65%) and p. a. hydrochloric acid ($\omega_{rel.}$(HCl) = 32%). For each iron coordination compound three individual samples were dissolved (triplicate determination) as well as blank digestions were performed to be able to correct for possible contaminations of the employed microwave tubes. After the digestion white and bulky insoluble (organic but demetallized) residues in the digestion solutions were removed by the use of metal-free syringe filters (*VWR*, Radnor, USA). The blank digestion solutions were treated in the same way to consider also possible iron impurities of the syringes and syringe filters. In a next step the received clear solutions were diluted with pure water for further ICP-OES analyses. The iron quantifications were done by an external 5-point calibration (ω(Fe) = 1 – 9 mg/kg). These standard solutions were prepared from a commercial iron stock solution (β(Fe) = 1000 mg/L, *Merck*) by dilution with pure water and also adding defined amounts of nitric acid and hydrochloric acid to get a similar matrix to the diluted sample solutions. In the ICP-OES analyses several selected iron lines (selection based on aspects such as predicted and observed sensitivities as well as interferences) were measured. The evaluation of the measurement results was done in accordance with DIN 38402-51[26] and DIN 32645 [27]. Subsequently, the evaluated single line results were checked for outliers via Grubbs´s test and averaged. In the end the determined iron contents of the three samples of each iron compound were also checked for outliers (Grubbs test) and averaged to get the overall results which are presented in Table S2 for three synthesized product charges. These charges were mainly used in the XAFS examinations in each case.

Table S2 ICP-OES iron quantification results given as percentage of mass of iron compared to theoretical values (assuming 100% purity). The belonging bias values were obtained by the application of bias propagation to evaluated confidence intervals. Presented are those three synthesized product charges (C1, C2 and C3) of each synthesized compound, which were mainly used in the XAFS experiments.

Sample	$\omega_{rel.}$**(Fe) / %**	$\omega_{rel.}$**(Fe) theor. / %**
$[Fe(bzimpy)_2](ClO_4)_2 \cdot 0.25\ H_2O$	C1: 6.06 ± 0.15	6.33
	C2: 5.94 ± 0.16	
	C3: 5.67 ± 0.17	
$[Fe(bzimpy_{-1H})_2] \cdot H_2O$	C1: 9.07 ± 0.17	8.04
	C2: 10.81 ± 0.18	
	C3: 8.00 ± 0.15	
FeTPP(Cl)	C1: 8.01 ± 0.12	7.93
	C2: 8.51 ± 0.14	experimental: 7.79 [15]
	C3: 7.46 ± 0.12	

The determined iron contents of the three iron compounds fitted to theoretical values (assuming the pure substances) in terms of the general scale in each case. But the deviations had to be explained. The iron concentrations in the charges of $[Fe(bzimpy)_2](ClO_4)_2 \cdot 0.25\ H_2O$ were somewhat lower than the calculated theoretical content. This can be explained by two aspects. Firstly, it is possible that the analyzed samples were not completely dried at the time of the ICP-OES analyses. Secondly, it has to be taken into account that the crystal water content of the compound can variate depending on the velocity of the product precipitation step. Contrary to the ideal and defined content of crystal water x = 0.25 variable values in the range of x < 1 are reported by Boča et al. 2001 [28]. Due to the fact of the rapid and fast precipitation method (solvent reduction + ice cooling) used in this work, this variable crystal water contents seemed probable. But this fact was not expected to be of a significant impact on the XAFS experiments. The iron contents of the analyzed $[Fe(bzimpy_{-1H})_2] \cdot H_2O$ charges, except charge no. 3 which fitted to the theory well, were slightly above the calculated concentrations. Here, a possible explanation could again be a divergent crystal water content (x < 1), but in this case no similar literature reports were found. Other possible reasons such as contaminations of obtained $[Fe(bzimpy_{-1H})_2] \cdot H_2O$ with residues of the educts or with other iron containing byproducts were mostly excluded due to the speciation results. The determined iron contents of the FeTPP(Cl) charges were different. Considering the received uncertainties charge no. 1 fitted to the calculated value well. However, charge 2 had a significant higher and charge 3 a lower iron concentration. In case of charge 2 an incomplete removal of the synthesis by-product iron(III) oxide and therefore in fact significant impurities were assumed. So, the XAFS measurements of this charge were of less informative value and are not presented in this work. The slightly lower iron content of charge 3 was explained by possible incomplete desiccations (solvent rests) as well as product precipitation in sort of a solvate. These aspects fitted to the also lower and explained FeTPP(Cl) iron content presented by Fleischer et al. 1971 [15] well. An also possible incomplete formation of the complex and therefore residues of the free ligand TPP were excluded in accordance to the already mentioned speciation results.

Particle size analysis

For particle sizes evaluation of the synthesized complex compounds the light microscope *Digital Microscope VHX 600* with zoom objective *VH-Z100UR* (*Keyence Corporation*, Osaka, Japan) was used. Very small sample amounts (few mg) were prepared on filter papers or alternatively on plane aluminum SEM sample holders pasted with a graphite pad and then examined with the mentioned microscope. The obtained results are shown in the Fig. S2a – c. The particle size analyses were done as a schematic overview in terms of the general rule that sample particle sizes have to be smaller than one absorption length ($d < \mu^{-1}$) to get optimal XAFS results [29].

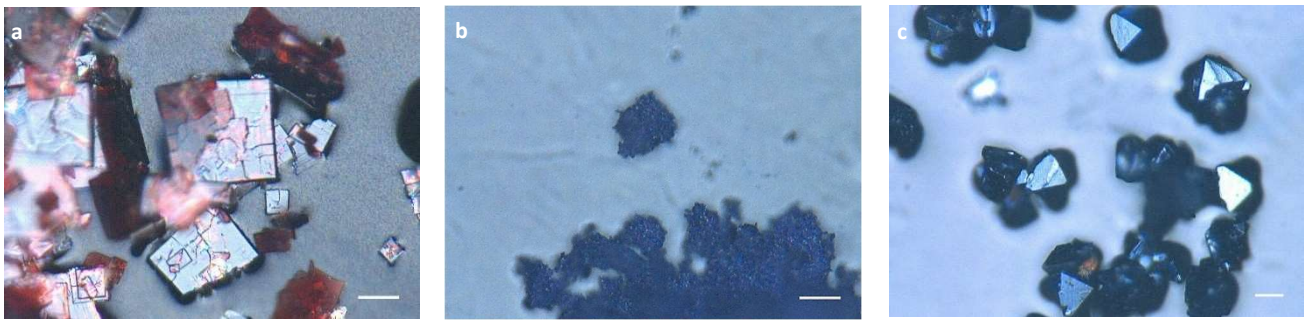

Fig. S2 Light microscopic images of the synthesized iron compounds – **a** $[Fe(bzimpy)_2](ClO_4)_2 \cdot 0.25\ H_2O$ (enlargement 1000x, scale bar d = 30 µm), **b** $[Fe(bzimpy_{-1H})_2] \cdot H_2O$ (enlargement 1000x, scale bar d = 30 µm), **c** FeTPP(Cl) (enlargement 700x, scale bar d = 30 µm). The pictures were taken immediately after the syntheses without further sample preparations. [16]

In case of $[Fe(bzimpy)_2](ClO_4)_2 \cdot 0.25\ H_2O$ (Fig. S2a) the largest particles / crystals found were at sizes of $d \approx 50 – 100$ µm. Due to the mentioned and measured low iron content even these comparatively large particles were in terms of the μ^{-1}-rule in a tolerable size range. Nevertheless, the samples were grounded in an agate mortar (under inter gas atmosphere) beforehand the XAFS preparation. This was necessary to obtain homogenous and especially stable (and not brittle) sample pellets, so the preparation method itself set the limit of particle sizes in this case. The particles of $[Fe(bzimpy_{-1H})_2] \cdot H_2O$ (Fig. S2b) were distinctly smaller than these of the protonated species. Just the formation of some loose agglomerates was observed, which were removed by slightly "stirring" (no real grounding) the sample in an agate mortar (also under inert gas) before the sample pellet preparation. The synthesized FeTPP(Cl) (Fig. S2c) mainly consisted of small crystals in sizes of $d \leq 50$ µm. These also were in the given μ^{-1}-rule particle size range and were just slightly grounded due to reasons of homogenous sample preparation.

Characterization of human hemoglobin

The sample human hemoglobin (Hb) sample was obtained from *Sigma Aldrich* in sort of a lyophilized, HIV- and HBV-free powder. In the course of a first macroscopic examination the delivered sample could be described as a fine crystalline, dark red to red-brown and soft solid which already fitted to the manufacturer information well. For a detailed characterization ICP-OES was used for elemental analysis, especially the determination of the iron content, and Bradford assay as well as SDS-PAGE (sodium dodecyl sulfate polyacrylamide gel electrophoresis) were done to determine the degree of species / protein purity. An additional particle size check with regard to the mentioned μ^{-1}-rule was not necessary due to the very low iron concentration of hemoglobin and the consequent theoretically tolerable very large particle sizes. In this case, just the XAFS preparation of the sample in sort of the pellet technique limited these sizes (otherwise, the obtained pellets would be inhomogeneous and would not even be stable). Nevertheless, the protein was grounded slightly beforehand the pellet preparation anyway.

The iron quantification by ICP-OES was done in a way very similar to that for the synthesized iron compounds mentioned above. Three samples of the human Hb (and one blank digestion) were taken and dissolved in aqua regia ($HCl : HNO_3 = 3 : 1$) by the same microwave assisted digestions system. After the removal of small amounts of insoluble residues by metal free syringe filters the digested samples were diluted with pure water for the following ICP-OES analyses. An external iron 5-point calibration (ω(Fe) = 150 – 300 µg/kg, prepared of the already mentioned iron stock solution by dilution with pure water and mixing with defined amounts of nitric acid and hydrochloric acid) was used and several iron lines were measured. The evaluation of the measurement results, the check for outliers, the results averaging of these lines as well as the final averaging (after an additional outlier check) to get the overall result were done in the same way as it has already been mentioned for the synthetic iron compounds.

Total protein quantification by Bradford assay was done by a prescription similar to these presented in Holtzhauer 1997 [30] and Reinard 2010 [31]. An external 6-point calibration based on BSA (bovine serum albumin) as standard (obtained from *Carl Roth*, $\omega_{rel.} \geq 98\%$, powder) was prepared in 1x PBS (phosphate-buffered saline) in the range of β(BSA) = 5 – 200 µg/mL. Every standard solution was prepared three times to compensate photometrical fluctuations by averaging the values. These solutions were mixed with 1 mL Bradford reagent (Bradford reagent, Roti-Quant, 5x concentrate, *Carl Roth*, diluted with water 1 : 5), incubated for 5 – 10 min and finally measured in polystyrene micro cuvettes (d = 1 cm, *Sarstedt*, Nümbrecht, Germany) at λ = 595 nm by the use of the photometer *UV-1600 PC Spectrophotometer* (*VWR*, Radnor, USA). Three samples of the human Hb were dissolved and further diluted with 1x PBS and treated and measured the same way as the standards. The evaluation

of these measurements was done in accordance with DIN 38402-51 [26] and DIN 32645 [27] and finally an averaging (after the Grubbs test to check for outliers) was done for getting the overall total protein content.
To determine the protein composition a SDS-PAGE was done at the Institute of Technical Chemistry Hannover. A human Hb stock solution (β(Hb) ≈ 1.5 mg/mL in 1x PBS) was prepared, further diluted with SDS sample buffer solution (two dilution stages were chosen: 1 : 2 and 1 : 4) and denatured (4 min at 95 °C followed by an ice cooling). The electrophoresis was performed in a 16% polyacrylamide gel with a running time of t = 2.5 h. Afterwards a direct silver staining without further blotting techniques was applied. To enable a qualitative assignment of the observed sample bands a protein size standard (*PageRuler Unstained Protein Ladder*, 10 – 200 kDa, *Thermo Fisher*, Waltham, USA) was analyzed in parallel in the same gel.

Table S3 shows the results of the human Hb characterizations. In case of the SDS-PAGE see Fig. S3 in addition.

Table S3 Overview of the human hemoglobin's characterization results compared to theoretical values and manufacturer information.

	Measured value	**Theoretical value**	**Manufacturer information** [32]
$\omega_{rel.}$ (Fe) / %	ICP-OES: 0.303 ± 0.009	≈ 0.35 (assuming pure desoxy Hb, M_r = 64.5 kDa)	0.25 – 0.35
Purity (species / protein)	Bradford assay (BSA standard): $\omega_{rel.}$ (total protein) = 94.62% ± 9.92% SDS-PAGE (16% gel, running time t = 2.5 h, silver staining): 4 bands observed - at M_r ≈ 64 kDa, 48 kDa, 32 kDa and 16 kDa – mostly electrophoretic pure	100%	≤ 15% H_2O, "pure"

The determined iron content fitted to the manufacturers specification [32], especially to the mentioned iron concentration range, very well. But the deviation to the value for the theoretical iron content also implies the presence of other minor components / impurities. The determination of the total protein content by Bradford assay demonstrated that the sample primary consisted of protein (considering the obtained uncertainties as well as general problems of the Bradford assay such as the use of BSA as a common universal standard and the dependence of color intensity on the structure and amino acid sequence composition of the sample protein [30]). In addition, the SDS-PAGE (Fig. S3) proved that this total protein content only consisted of hemoglobin, because solely the typical four bands of the different denaturation stages of Hb (tetramer, trimer, dimer and monomer) were observed in a significant intensity (at least at the selected two dilution stages of the sample).

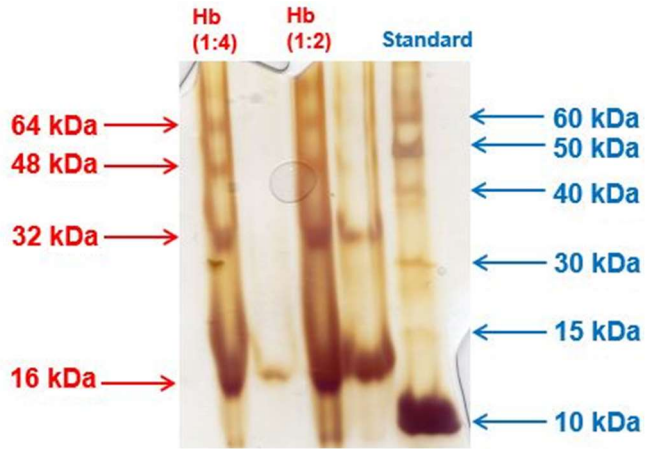

Fig. S3 SDS-PAGE of the human hemoglobin sample (16% gel, running time t = 2.5 h, silver staining) – The two sample dilution stages (1:2 and 1:4) (red) are shown in comparison to the protein size standard (blue). Also, there are bands in the gel pocket between the Hb 1:2 and the standard observable, because a small amount of the Hb sample solution ran over into this empty pocket during the gel loading. [16]

In accordance with the manufacturer information it was concluded that the major impurity of the human hemoglobin sample was simply (absorbed or / and adsorbed) water, which should not strongly affect the XAFS spectra. Therefore the measured iron content was just used to estimate the hemoglobin sample amounts for the XAFS pellet preparation.

Determination of the edge position E_0 and pre-edge peak fitting

The determination of the edge position E_0 was defined at 50% of the jump in the normalized spectra. The pre-edge peak centroid was determined by fitting the pre-edge peak with the *Larch* software package.[33] As the model a Voigt peak with previous baseline fitting was used. For all the XAFS spectra obtained by either laboratory (Lab) or at the synchrotron radiation facility ESRF (SR) the same fitting model was used (Fig. S4 – S5). The results of edge position E_0 and centroid position of the pre-edge peak are listed in Table S4. The result for the centroid position of the Lab-XAFS spectra of Hemoglobin is not reliable due to the low signal to noise ratio. The uncertainty of the edge position results from the minimal energy step while the uncertainty for the centroid position is given by the standard deviation by the peak fitting procedure.

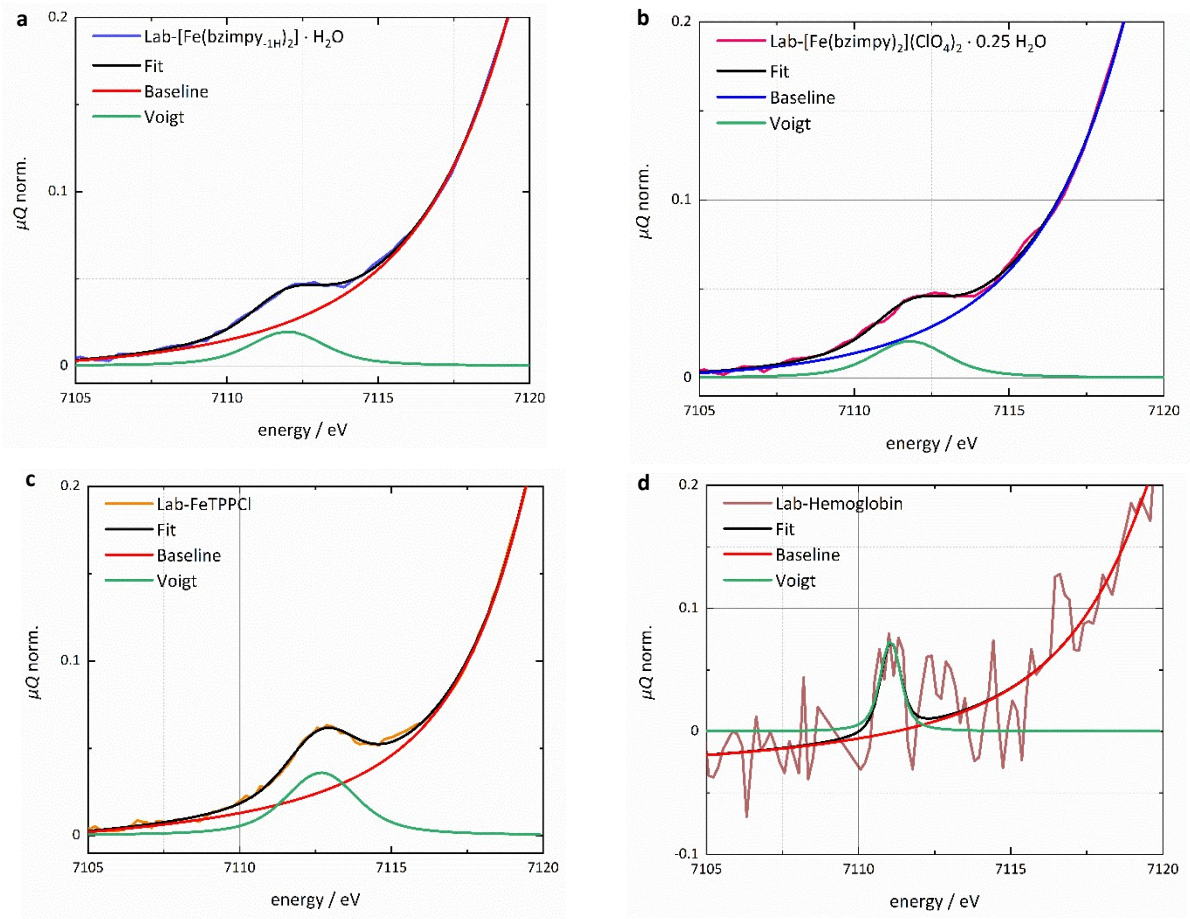

Fig. S4 Pre-edge region of the normalized Lab-XAFS-spectra with pre-edge fit for determine the centroid position. **a** [Fe(bzimpy)$_2$](ClO$_4$)$_2$ · 0.25 H$_2$O, **b** [Fe(bzimpy$_{-1H}$)$_2$] · H$_2$O , **c** FeTPP(Cl), **d** Hemoglobin. The fitting was done by using the *Larch* software package [33]. The same fitting model is used for all four pre-edge peaks as well for the SR-XAFS spectra in Fig. S5. The fit and therefore the result for the centroid position of the Lab Hemoglobin is not reliable due to the high signal to noise ratio. The centroid positions are listed in Table S4.

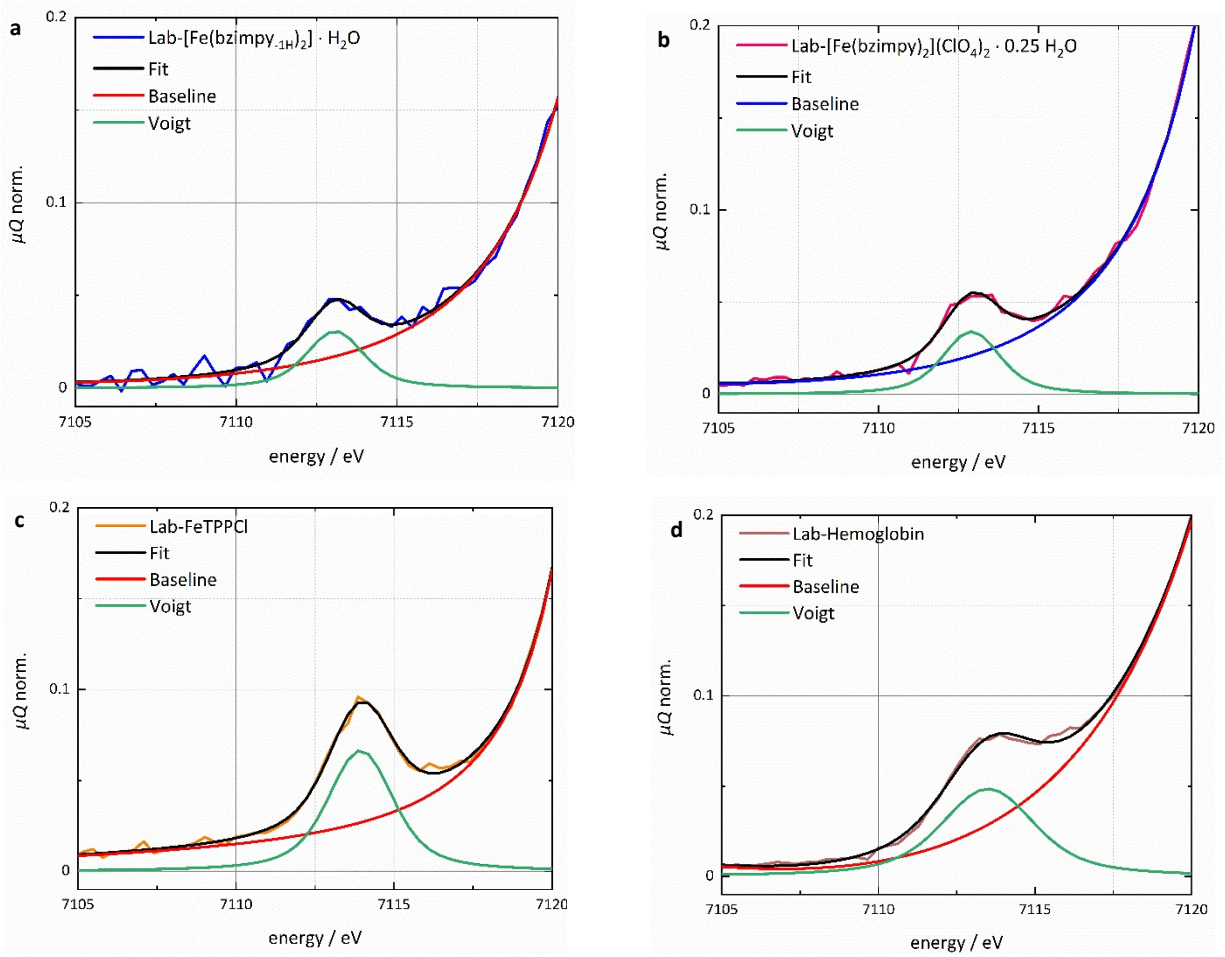

Fig. S5 Pre-edge region of the normalized synchrotron radiation (SR-)XAFS-spectra with pre-edge fit for determine the centroid position. **A** [Fe(bzimpy$_{-1H}$)$_2$] · H$_2$O, **b** [Fe(bzimpy)$_2$](ClO$_4$)$_2$ · 0.25 H$_2$O, **c** FeTPP(Cl), **d** Hemoglobin. The fitting was done by using the *Larch* software package [33]. The same fitting model is used for all four pre-edge peaks, as well for the Lab-XAFS spectra in Fig. S4.

Table S4 Iron K-edge position E_0 and pre-edge peak centroid, obtained by fitting with the *Larch* software package [33], of the examined samples. The result for the centroid position of the Lab-XAFS of Hemoglobin (highlighted in red) is not reliable due to the high signal to noise ratio, which can be seen in Fig. S4d. The uncertainty for E_0 is given by the minimal energy step. The centroid position uncertainty is the standard deviation obtained by the peak fitting procedure.

Sample	E_0 / eV	Pre-edge centroid / eV
[Fe(bzimpy)$_2$](ClO$_4$)$_2$ · 0.25 H$_2$O	**Lab** = 7121.8 ± 0.5	**Lab** = 7111.79 ± 0.08
	SR = 7122.6 ± 0.5	SR = 7112.90 ± 0.06
[Fe(bzimpy$_{-1H}$)$_2$] · H$_2$O	**Lab** = 7122.6 ± 0.5	**Lab** = 7112.0 ± 0.6
	SR = 7123.6 ± 0.5	SR = 7113.1 ± 0.1
FeTPP(Cl)	**Lab** = 7122.2 ± 0.5	**Lab** = 7112.68 ± 0.03
	SR = 7122.8 ± 0.5	SR = 7113.94 ± 0.03
Hemoglobin	**Lab** = 7123.0 ± 0.5	**Lab** = 7111.1 ± 0.1
	SR = 7123.2 ± 0.5	SR = 7113.50 ± 0.05

List of chemicals

Acetone (CH_3COCH_3), $\omega_{rel.} \geq 99{,}5\%$, for synthesis, *Carl Roth*
Albumin Fraction V (Bovine Serum Albumin, BSA), $\omega_{rel.} \geq 98\%$, powder, for Molecular biology, *Carl Roth*
Ammonia solution ($NH_{3(aq)}$), $\omega_{rel.} = 30 – 33\%$, pure, *Carl Roth*
Argon (Ar)
(L)-(+)-ascorbic acid ($C_6H_8O_6$), ≥ 99%, p. a., *Carl Roth*
Benzaldehyde (C_7H_6O), ≥ 99%, ReagentPlus®, *Sigma-Aldrich*
Bradford reagent, Roti®-Quant, 5x concentrate, *Carl Roth*
Calcium chloride ($CaCl_2$), ≥ 93,0%, anhydrous, granules, $d \leq 7{,}00$ mm, *Sigma-Aldrich*
Charcoal, p. a., powder, *Carl Roth*
Chloroform, deuterated (Chloroform-D, $CDCl_3$), 99,8%, *deutero*
2,3-Dichloro-5,6-dicyano-1,4-benzoquinone (DDQ, $C_8Cl_2N_2O_2$), 98%, *Sigma-Aldrich*
Dichloromethane (DCM, CH_2Cl_2), ≥ 99,5%, for synthesis, *Carl Roth*
N, N-Dimethylformamide (DMF, C_3H_7NO), ≥ 99,5%, for synthesis, *Carl Roth*
Dimethyl sulfoxide, deuterated (DMSO-D_6, C_2D_6OS), 99,8%, *deutero*
Dry pearls, Silica
Ethanol (EtOH, CH_3CH_2OH), $\omega_{rel} \geq 99{,}8\%$, denatured with ca. 1% MEK, *Carl Roth*
Human hemoglobin (Hb), lyophilized powder, $\omega_{rel.(Fe)} = 0{,}25 – 0{,}35\%$, ≤ 15% H_2O, HIV-/ HBV-tested negative, *Sigma-Aldrich*
Hydrochloric acid ($HCl_{(aq)}$), $\omega_{rel.(HCl)} = 32\%$, p. a., Emsure®, *Merck*
Hydrochloric acid ($HCl_{(aq)}$), $\omega_{rel.(HCl)} = 32\%$, p. a., Rotipuran®, ISO, *Carl Roth*
Hydrochloric acid ($HCl_{(aq)}$), fuming, $\omega_{rel.(HCl)} = 37\%$, p. a., Emsure®, *Merck*
Hydrogen peroxide ($H_2O_{2(aq)}$), $\omega_{rel.(H_2O_2)} = 30\%$, Rotipuran®, p. a., ISO, stabilized, *Carl Roth*
Iron(II) chloride tetrahydrate ($FeCl_2 \cdot 4\ H_2O$), 98%, ReagentPlus®, *Sigma-Aldrich*
Iron(II) chloride tetrahydrate ($FeCl_2 \cdot 4\ H_2O$), ≥ 99,0%, puriss. p. a., *Sigma-Aldrich*
Iron(II) perchlorate hydrate ($Fe(ClO_4)_2 \cdot x\ H_2O$), 98%, *Sigma-Aldrich*
Iron stock solution, $\beta(Fe) = 1000$ mg/L, $Fe(NO_3)_3$ in 0,5 M HNO_3, Certipur®, *Merck*
Methanol (MeOH, CH_3OH), ≥ 99,8% (GC), puriss. p. a., ACS reagent, *Sigma-Aldrich* & *Merck*
Methanol (MeOH, CH_3OH), Rotisolv® HPLC Gradient, *Carl Roth*
Nitric acid ($HNO_{3(aq)}$), $\omega_{rel.(HNO_3)} = 65\%$, sub boiled from p. a., Emsure®, *Merck*
o-Phenylene diamine ($C_6H_8N_2$), 99,5%, Flakes, *Sigma-Aldrich*
Polyphosphoric acid (PPA, $H_{n+2}P_nO_{3n+1}$), 105%- & 115% base, reagent grade, *Sigma-Aldrich* & *Honeywell* / *Fluka*
Potassium chloride (KCl), pure, *Merck*
Propane acid (Propionic acid, CH_3CH_2COOH), ≥ 99,5%, reagent grade, *Sigma-Aldrich* & *Honeywell* / *Fluka*
Protein size standard, PageRuler unstained Protein Ladder, 10 – 200 kDa, *Thermo Scientific*
2,6-Pyridine dicarboxylic acid ($C_7H_5NO_4$), 99%, *Sigma-Aldrich*
Pyrrole (C_4H_5N), 98%, reagent grade, *Sigma-Aldrich*
SDS electrophoresis buffer (25 mM Tris, 192 mM Glycine, 0,1% SDS, pH = 8,3)
SDS sample buffer (20 mM Tris/HCl, 2 mM Na-EDTA, 5% SDS, 0,02% bromophenol blue in 90 mL H_2O → before using: + 10% 2-mercapto ethanol, 10% glycerin)
SDS stacking gel (Polyacrylamide/ Bisacrylamide, SDS, Tris/HCl (1,5 M, pH = 6,8), TEMED, APS)
SDS running gel (Polyacrylamide/ Bisacrylamide, SDS, Tris/HCl (1,5 M, pH = 8,8), H_2O: 3,3, TEMED, APS)
SDS silver staining solutions
Sodium chloride (NaCl), pure, *Merck*
Sodium dihydrogen phosphate hydrate ($NaH_2PO_4 \cdot H_2O$), for analysis, *Merck*
Sodium dithionite ($Na_2S_2O_4$), ≥ 82%, *Sigma-Aldrich*
Sodium hydrogen phosphate dihydrate ($Na_2HPO_4 \cdot 2\ H_2O$), for analysis, *Merck*
Sodium hydroxide (NaOH), ≥ 99%, p. a., ISO, tablets, *Carl Roth*
Sodium sulfate (Na_2SO_4), ≥ 99,0%, ACS reagent, anhydrous, granules, *Sigma-Aldrich*
meso-Tetraphenylporphyrin (TPP, $C_{44}H_{30}N_4$), ≥ 99%, *Sigma-Aldrich*
meso-Tetraphenylporphyrin (TPP, $C_{44}H_{30}N_4$), ≥ 99,0% (HPLC), *Sigma-Aldrich*
Toluene (C_7H_8), ≥ 99,5%, for synthesis, *Carl Roth*
Triethylamine (TEA, $C_6H_{15}N$), ≥ 99%, *Sigma-Aldrich*
Water (H_2O), high-purity
Xylene (C_8H_{10}), mixed isomers, reagent grade, *Sigma-Aldrich*

References

1 A. W. Addison and P. J. Burke, Synthesis of some imidazole- and pyrazole- derived chelating agents, *Journal of Heterocyclic Chemistry*, 1981, **18**, 803–805.

2 G. Li, J. Huang, M. Zhang, Y. Zhou, D. Zhang, Z. Wu, S. Wang, X. Weng, X. Zhou and G. Yang, Bis(benzimidazole)pyridine derivative as a new class of G-quadruplex inducing and stabilizing ligand, *Chemical communications (Cambridge, England)*, 2008, 4564–4566.

3 R. Boča, P. Baran, L. Dlháň, H. Fuess, W. Haase, F. Renz, W. Linert, I. Svoboda and R. Werner, Crystal structure and spin crossover studies on bis(2,6-bis(benzimidazol-2-yl)pyridine) iron(II) perchlorate, *Inorganica Chimica Acta*, 1997, **260**, 129–136.

4 R. Boča, F. Renz, M. Boča, H. Fuess, W. Haase, G. Kickelbick, W. Linert and M. Vrbová-Schikora, Tuning the spin crossover above room temperature: iron(II) complexes of substituted and deprotonated 2,6-bis(benzimidazol-2-yl)pyridine, *Inorganic Chemistry Communications*, 2005, **8**, 227–230.

5 B. Strauß, W. Linert, V. Gutmann and R. F. Jameson, Spin-crossover complexes in solution, I. Substitutional lability of $[Fe(bzimpy)_2](ClO_4)_2$, *Monatsh Chem*, 1992, **123**, 537–546.

6 B. Strauß, V. Gutmann and W. Linert, Spin-crossover complexes in solution, II solvent effects on the high spin-low spin-equilibrium of $[Fe(bzimpy)_2](ClO_4)_2$, *Monatsh Chem*, 1993, **124**, 515–522.

7 A. D. Adler, F. R. Longo, J. D. Finarelli, J. Goldmacher, J. Assour and L. Korsakoff, A simplified synthesis for meso-tetraphenylporphine, *J. Org. Chem.*, 1967, **32**, 476.

8 K. M. Smith, in *The Porphyrin Handbook Vol. 1 - Synthesis and organic chemistry*, ed. K. M. Kadish, K. M. Smith and R. Guilard, Academic Press, San Diego, Calif., 2000, Chapter 1: Strategies for the Synthesis of Octaalkylporphyrin Systems, pp. 1–43.

9 J. S. Lindsey, in *The Porphyrin Handbook Vol. 1 - Synthesis and organic chemistry*, ed. K. M. Kadish, K. M. Smith and R. Guilard, Academic Press, San Diego, Calif., 2000, Chapter 2: Synthesis of meso-Substituted Porphyrins, pp. 45–118.

10 J. S. Lindsey, I. C. Schreiman, H. C. Hsu, P. C. Kearney and A. M. Marguerettaz, Rothemund and Adler-Longo reactions revisited: synthesis of tetraphenylporphyrins under equilibrium conditions, *J. Org. Chem.*, 1987, **52**, 827–836.

11 Z.-C. Sun, Y.-B. She, Y. Zhou, X.-F. Song and K. Li, Synthesis, characterization and spectral properties of substituted tetraphenylporphyrin iron chloride complexes, *Molecules (Basel, Switzerland)*, 2011, **16**, 2960–2970.

12 G. H. Barnett, M. F. Hudson and K. M. Smith, Concerning meso-tetraphenylporphyrin purification, *J. Chem. Soc., Perkin Trans. 1*, 1975, 1401–1403.

13 K. Rousseau and D. Dolphin, A purification of meso-tetraphenylporphyrin, *Tetrahedron Letters*, 1974, **15**, 4251–4254.

14 A. D. Adler, F. R. Longo, F. Kampas and J. Kim, On the preparation of metalloporphyrins, *Journal of Inorganic and Nuclear Chemistry*, 1970, **32**, 2443–2445.

15 E. B. Fleischer, J. M. Palmer, T. S. Srivastava and A. Chatterjee, Thermodynamic and kinetic properties of an iron-porphyrin system, *J. Am. Chem. Soc.*, 1971, **93**, 3162–3167.

16 D. A. Motz, *Entwicklung von Referenzmaterialien für die Röntgen-Nahkanten-Absorptionsspektroskopie am Laboraufbau*, Hannover : Institutionelles Repositorium der Leibniz Universität Hannover, 2021.

17 D. O. Cheng and E. LeGoff, Synthesis of substituted porphyrins, *Tetrahedron Letters*, 1977, **18**, 1469–1472.

18 C. Janiak, in *Moderne Anorganische Chemie*, ed. E. Riedel, C. Janiak, T. Klapötke and H.-J. Meyer, Walter de Gruyter, 2007, Chapter 3: Komplex-/ Koordinationschemie, pp. 381–579.

19 L. H. Gade, *Koordinationschemie*, Wiley-VCH, Weinheim, 1st edn., 1998.

20 L. Beyer and J. Angulo Cornejo, *Koordinationschemie*, Vieweg+Teubner Verlag, Wiesbaden, 2012.

21 F. A. Miller and C. H. Wilkins, Infrared spectra and characteristic frequencies of inorganic ions, *Anal. Chem.*, 1952, **24**, 1253–1294.

22 J. B. Kim, J. J. Leonard and F. R. Longo, A mechanistic study of the synthesis and spectral properties of meso-tetraarylporphyrins, *J. Am. Chem. Soc.*, 1972, **94**, 3986–3992.

23 M. Lan, H. Zhao, H. Yuan, C. Jiang, S. Zuo and Y. Jiang, Absorption and EPR spectra of some porphyrins and metalloporphyrins, *Dyes and Pigments*, 2007, **74**, 357–362.

24 W. D. Edwards, B. Weiner and M. C. Zerner, On the low-lying states and electronic spectroscopy of iron(II) porphine, *J. Am. Chem. Soc.*, 1986, **108**, 2196–2204.

25 W. Zheng, N. Shan, L. Yu and X. Wang, UV–visible, fluorescence and EPR properties of porphyrins and metalloporphyrins, *Dyes and Pigments*, 2008, **77**, 153–157.

26 *DIN 38402-51:1986 – Kalibrierung von Analyseverfahren, Auswertung von Analysenergebnissen und lineare Kalibrierfunktionen für die Bestimmung von Verfahrenskenngrößen*, Deutsches Institut für Normung.

27 *DIN 32645:2008-11, Chemische Analytik- Nachweis-, Erfassungs- und Bestimmungsgrenze unter Wiederholbedingungen- Begriffe, Verfahren, Auswertung*, Deutsches Institut für Normung, Berlin.

28 R. Boča, M. Boča, L. Dlhán, K. Falk, H. Fuess, W. Haase, R. Jarosciak, B. Papánková, F. Renz, M. Vrbová and R. Werner, Strong cooperativeness in the mononuclear iron(II) derivative exhibiting an abrupt spin transition above 400 K, *Inorg. Chem.*, 2001, **40**, 3025–3033.

29 G. Bunker, *Introduction to XAFS*, Cambridge University Press, Cambridge, 2010.

30 M. Holtzhauer, *Biochemische Labormethoden*, Springer Berlin Heidelberg, Berlin, Heidelberg, 1997.
31 T. Reinard, *Molekularbiologische Methoden*, Ulmer, Stuttgart, 1st edn., 2010.
32 Sigma-Aldrich, *Hämoglobin human (H7379),* www.sigmaaldrich.com/DE/de/product/sigma/h7379, (accessed 14 December 2021).
33 M. Newville, Larch: An Analysis Package for XAFS and Related Spectroscopies, *J. Phys.: Conf. Ser.*, 2013, **430**, 12007.